

First Principles Calculation of Localized Surface Phonons and Electron-Phonon Interaction at Pb(111) Thin Films

Felix Yndurain*

*Departamento de Física de la Materia Condensada and Instituto de Ciencia de Materiales “Nicolás Cabrera”,
Universidad Autónoma de Madrid, Cantoblanco, 28049 Madrid, Spain*

Manuel Perez Jigato

Departamento de Física de la Materia Condensada, Universidad Autónoma de Madrid, Cantoblanco, 28049 Madrid, Spain
(Received 3 December 2007; published 21 May 2008)

A first principles calculation of the vibrational modes of Pb(111) thin films of thickness up to 14 layers reveals the existence of localized vibrational modes at the slab’s surface. Both longitudinal and transverse surface modes localized a few atomic layers are found at energies above the bulk bands. The frequency of these modes presents a bilayer oscillatory behavior. The electron-phonon interaction of the slab’s quantum well states is also calculated. We find a large (small) deformation potential for the lowest unoccupied (highest occupied) quantum well state. Its absolute value is also oscillatory with the number of layers.

DOI: [10.1103/PhysRevLett.100.205501](https://doi.org/10.1103/PhysRevLett.100.205501)

PACS numbers: 63.22.Np, 63.20.dk, 68.65.Fg, 74.25.Kc

The possibility of growing Pb(111) thin films on top of different substrates in a layer by layer regime in a controlled way (see [1,2] and references therein) has opened the possibility of tuning different physical properties with the thin film size. Previous work has shown that quantum size effects, in particular, quantum well states (QWS), play a crucial role in the physical properties of these slabs. Electrical resistivity [3], Hall coefficient [4], work function [5], roughening temperature [6] etc. show a periodic oscillatory variation with the number of layers with a bilayer periodicity. Oscillations in the interlayer distances have been recently reported [1] and the equilibrium height distribution of islands [7] has been discussed along the same lines. These oscillations can be understood by the confinement of the free electrons in the slabs (for details see [8]), the periodicity being due to the charge oscillation governed by the Fermi wavelength λ_F . More recently, superconductivity in slabs has been well established experimentally [9,10] and the possibility the superconducting critical temperature T_C displaying oscillatory behavior with the slab thickness has been proposed based on experimental tunneling data [11,12] and treated theoretically by Shanenko *et al.* [13]. Similarly, the electron-phonon coupling constant (λ) appears to oscillate with the number of Pb(111) layers in the slab [14].

We have studied, from first principles, the phonon spectra of Pb(111) slabs of different thickness. To obtain the phonons we have calculated the forces acting on the atoms, after small deviations of the atoms with respect to their equilibrium configuration. The forces are calculated through the Hellmann-Feynman theorem. The total energy calculations are based on the density functional theory (DFT)[15,16]. To solve the Kohn-Sham self-consistent equations we use Vienna *ab initio* simulation package (VASP) [17,18]. We use the functional of Perdew and Wang [19] to approximate the exchange-correlation within

the generalized gradient approximation. Ultrasoft pseudo-potentials [20] are used such that only *s* and *p* electrons are included in the valence band. Special care has been taken to obtain good convergence with respect to reciprocal and real space sampling, energy cutoff, self-consistency convergence criteria, etc. We perform an “accurate” calculation avoiding wraparound errors [17,18]. The energy cutoff is 200 eV, the number of *k* points in the two-dimensional Brillouin zone is 961 in the Monkhorst Pack distribution and the energy convergence criteria in the self-consistent loop is 10^{-6} eV. Because of the discrete character of the QWS, we have used the Methfessel and Paxton [21] smearing method. The layers are relaxed to minimize the equilibrium forces down to less than 0.01 eV/Å. We have obtained for bulk fcc a lattice constant of 5.03 Å in reasonable agreement with the 4.95 Å experimental value.

The phonon dispersion relation of bulk Pb-fcc is first calculated as a check of our method of calculation. Lead is a soft material such that its phonon spectrum [22] has anomalies which in turn are related to Fermi surface features.

To calculate phonon’s dispersion relations in any arbitrary direction requires very large unit cells making a reliable calculation difficult. However, to get the dispersion relation along symmetry directions, we have constructed unit cells formed by a few atomic planes. In this way to obtain the dispersion relations along the (111) and (100) *k* space directions we have considered fcc lattice unit cells containing a given number of (111) and (100) planes and calculated the phonon frequencies at $k = 0$. If we take, say, *N* layers separated by an interlayer spacing “*a*”, the allowed *k* values within the conventional fcc Brillouin zone are given by $k_n = \frac{2\pi}{Na}n$ with $n = 0, 1, 2, \dots, \frac{N}{2}$. This procedure, within the DFT total energy calculation, provides an “exact” result since, for the selected vibrational modes, only the calculated forces between the atoms in the unit

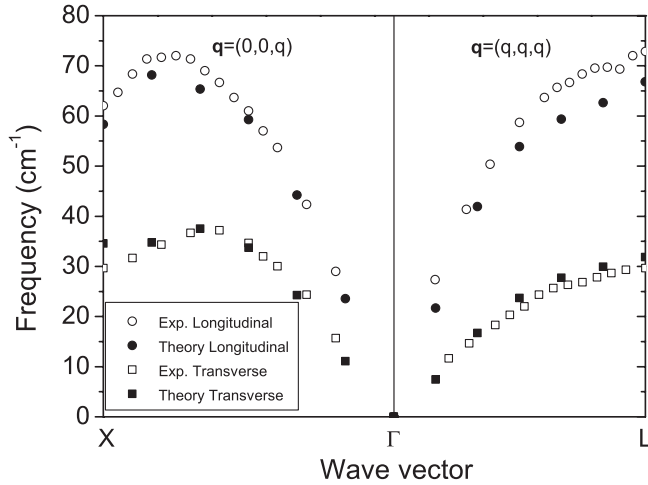


FIG. 1. Calculated and experimental (Ref. [22]) data of vibrational modes of bulk Pb along the symmetry directions (001) and (111) for unit cells containing 12 layers (see text). Bold (open) symbols stand for theoretical (experimental) results. Circles and squares stand for longitudinal and transverse modes, respectively.

cell are those involved. The results of the phonon dispersion calculation for $N = 12$ are given in Fig. 1. We obtain a good agreement with experiments similar to previous calculations [23,24] using linear response theory.

Zero parallel momentum phonon modes have been calculated for Pb(111) freestanding slabs of widths ranging from 3 to 14 layers. Before performing the phonon calculation we have relaxed the structures such that the forces acting on all the atoms be smaller than $0.01 \text{ eV}/\text{\AA}$. We [8], like previous calculations [25,26], obtain a bilayer oscillatory behavior of the slab thickness with a “beating” every 10 layers; see Fig. 2(c). We consider unit cells of the required number of layers separated by an empty space. The vacuum between the slabs is large enough (of the order of 11 \AA) to avoid interaction between the slabs. Results of the localized phonon modes in the different layers are shown in Fig. 2.

Both longitudinal and transverse surface modes take place at energies above the corresponding bulk values (see Fig. 1) due to a 6% contraction of the surface layer. In the case of the longitudinal modes we have performed the calculations in two different ways to assess how the results are substrate independent: in one case we allow all the atoms in the slabs to move; we then find localized modes at both slabs surfaces. These modes (with the same frequency in a hypothetical infinite slab) interact having then different frequencies. This splitting is smaller the wider the slab. In another calculation, the atom at one slab surface is kept fixed obtaining only one localized mode at the free surface with a frequency intermediate between those of the free ends slab. A bilayer oscillatory variation of both surface states is found (Fig. 2), being more pronounced for the longitudinal modes than in the transverse ones as expected due to their different character.

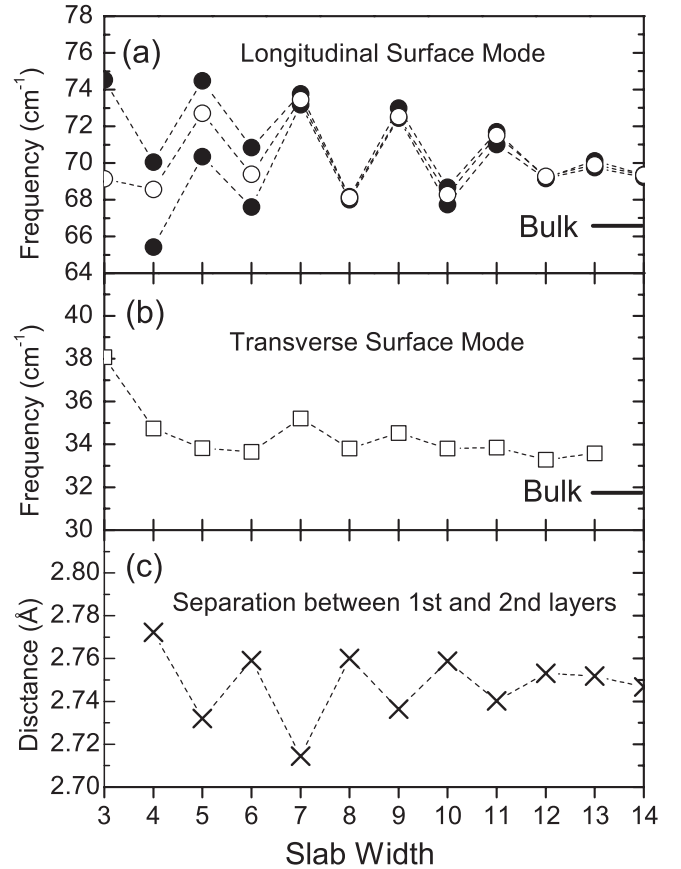


FIG. 2. Frequencies of localized surface phonon modes at $k_{\parallel} = 0$ for different slab thicknesses (see text). Panels (a) and (b) stand for longitudinal and transverse modes, respectively. In both cases the highest corresponding bulk mode frequency is indicated. In panel (a) the results considering the cases of both slab’s ends free (bold symbols) and fixing one while leaving the other one free (open symbols) are shown. Panel (b) stands only for the case of one slab’s ends fixed. Panel (c) shows the contraction of the outermost layer. The bulk layer separation is 2.91 \AA .

Presumably, localized modes at the surface will be present in a semi-infinite crystal as well. In Table I we give the values of the matrix elements of the dynamical matrix D between the different layers in the case of a 12 layer slab and in the bulk such that $D_{i\alpha,j\beta} = \frac{1}{M} \frac{\partial^2 E}{\partial u_{i\alpha} \partial u_{j\beta}}$, where i, j stands for the atom, $\alpha, \beta = x, y, z$, M is the atom mass, E is the total energy, and u is the displacement of the corresponding atom. We immediately observe the stronger forces between first and second layers in the slabs responsible of the localized surface mode. The local character of the surface perturbation is apparent, the matrix elements at the fourth layer are almost identical to the bulk ones.

For a proper characterization of the localized surface longitudinal mode we show in Fig. 3 (for several slabs sizes) the displacement of the different atoms in the presence of the longitudinal localized mode. The mode is also compared with the highest bulk mode at the L point of the Brillouin zone (see Fig. 1). The local character of the mode

TABLE I. Dynamical matrix elements near the surface and in the bulk. Only displacements in the direction z perpendicular to the surface are considered. Label n stands for layer index in the slab. Label 1 is the surface layer, label 2 is the layer underneath and so on. The bulk values are obtained with a 12-layers unit cell along the (111) direction in the fcc lattice.

	Surface	Surface	Surface	Surface	Bulk
n	$D_{1z,nz}$	$D_{2z,nz}$	$D_{3z,nz}$	$D_{4z,nz}$	$D_{4z,nz}$
1	-0.033	0.030	0.002	0.002	0.001
2	0.030	-0.046	0.012	0.003	0.003
3	0.002	0.012	-0.034	0.016	0.015
4	0.002	0.003	0.016	-0.038	-0.038
5	-0.002	0.002	0.003	0.014	0.015
6	0.0	0.0	0.0	0.003	0.003
7	0.0	0.0	0.0	0.0	0.001

is apparent, its character and amplitude being almost independent of the slab size.

We have calculated the deformation potential of different electronic energy levels in the presence of the surface longitudinal mode. In Fig. 4 we show the effect of the mode in the electronic energy bands in the case of a 10 Pb(111) layers slab. The presence of the vibrational mode affects in a different way the QWS near $k_{\parallel} = 0$; when the wavelength of the quantum well state, $\lambda_n = 2 \times n \times L$, is much larger than the localization of the surface phonon mode, the vibrational mode does not affect the energy of the corresponding electronic state, only when λ_n is comparable with the phonon wavelength (see Fig. 3), the interaction is strong. Mostly the unoccupied quantum well states are affected by the phonon distortion. In Fig. 4 we also show

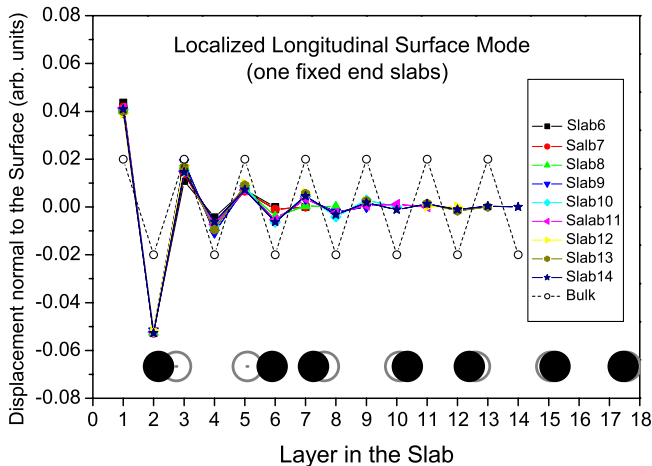


FIG. 3 (color online). Displacement of the atoms in the presence of the localized longitudinal surface vibrational mode (Fig. 2). The displacement is in arbitrary units. The different data stand for different size slabs. In all cases the other slab end was kept fixed. The longitudinal optical bulk mode at the L point of the Brillouin zone is also shown (open symbols). The inset shows a schematic motion of the planes (black circles) in the presence of the surface vibrational mode. Open circles stand for the equilibrium positions.

the variation of the total energy with the longitudinal surface phonon amplitude; a fourth order polynomial fit for the slabs with 9 and 8 layers gives $E = 8162(\Delta u)^2 + 10342(\Delta u)^3 + 24226(\Delta u)^4$ and $E = 7160(\Delta u)^2 + 11327(\Delta u)^3 + 13594(\Delta u)^4$, respectively, where the energy is in meV and the Δu in Å. This indicates small deviations from harmonicity for small phonon amplitudes; for instance for a 0.02 Å phonon amplitude the cubic term is of the order of a 3% of the quadratic contribution. We have estimated the deformation potential considering the deviation of the energy level with the presence of a mode. In this way, the deformation potential α is given by $\alpha = \Delta E/\Delta u$, where ΔE is the energy level shift induced by a phonon of amplitude Δu . In Fig. 5 we show the variation with the number of layers in the slab of the quantum well states closest to the Fermi level. We obtain a strong and oscillatory behavior for lowest unoccupied molecular orbital (LUMO), and a weak and nonoscillatory behavior for highest occupied molecular orbital (HOMO) that can be measured by means of scanning tunneling spectroscopy.

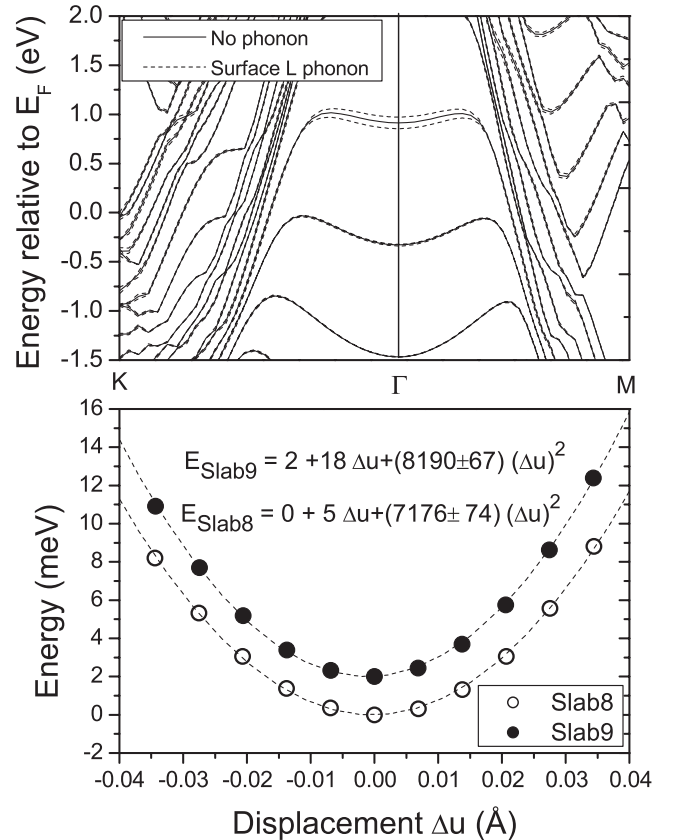


FIG. 4. Effects of the longitudinal surface mode on the electronic structure. The upper panel shows the band structure of a 10 layers slab. Solid lines are the bands without the phonon and broken lines represent the bands in the presence of the phonon with a generalized coordinate amplitude (root mean square displacement) of 0.034 Å. Lower panel represents the variation of the total energy with the phonon's amplitude. The curves have been shifted 2 meV for clarity sake. The broken lines are second order polynomial fits to the total energy data.

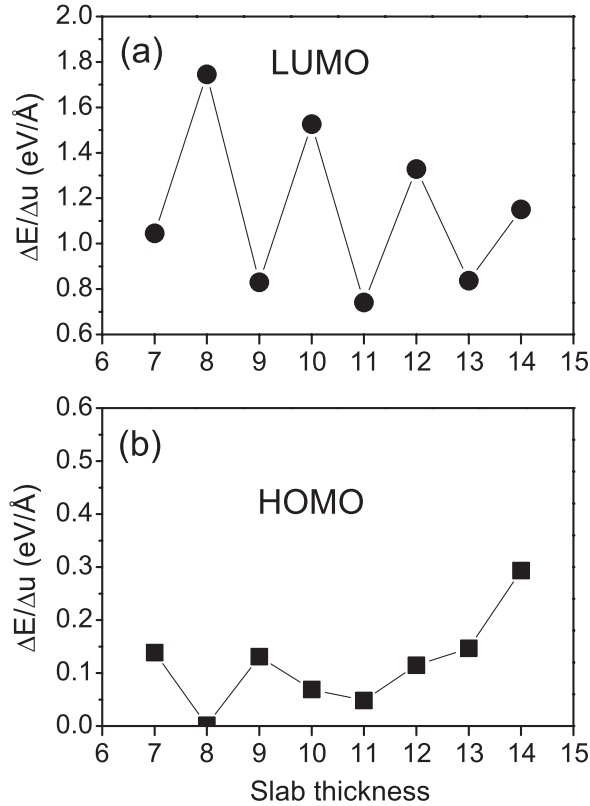


FIG. 5. Slab width dependence of the deformation potential (see text) of the quantum well states at $k_{\parallel} = 0$ in the presence of the longitudinal surface phonon mode. Panels (a) and (b) show the results for the LUMO and HOMO energy levels.

Whether or not this behavior would induce a oscillatory bilayer variation of the superconducting critical temperature would require to extend this calculation to all phonons and all electronic states, which is far beyond the scope of this work. We, however, believe that, as far as the *oscillatory* behavior of T_C is concerned, the analyzed surface phonon mode is the most relevant since it is related to the slab width and is coupled to the QWS which, in turn, are responsible for the oscillatory variation of many other physical properties.

To summarize, first principles calculation has allowed us to conclude the following. (i) Finite (and presumably semi-infinite) Pb(111) slabs have localized surface phonons at frequencies above the bulk highest value. Although only phonons at $k_{\parallel} = 0$ are calculated, they should be present in a large portion of the two-dimensional Brillouin zone like the almost dispersionless surface phonons in the Ru(0001) surface [27]. (ii) In the case of freestanding slabs these surface modes interact giving rise to two modes (localized at either surface) with different frequencies. (iii) The frequency of these modes has an oscillatory behavior with a bilayer periodicity. (iv) The electronic QWS states broadening due to the electron-phonon interaction depends very much on the character of the QWS considered. (v) The electron-phonon interaction of the lowest unoccupied

QWS has also an oscillatory variation with a bilayer periodicity.

We are indebted to E. Anglada, G. Gomez-Santos, R. Miranda, P. Segovia, and J. M. Soler for helpful discussions and to O. Paz for critical reading of the manuscript. Financial support of the Ministry of Education and Science through grant No. BFM2003-03372 and Madrid's Comunidad Autonoma through grant Nanomagnet No. S-0505/MAT/0194 are acknowledged.

*felix.yndurain@uam.es.

- [1] P. Czochke, H. Hong, L. Basile, and T.-C. Chiang, Phys. Rev. Lett. **91**, 226801 (2003).
- [2] D.-A. Luh, T. Miller, J. Paggel, M. Chou, and T.-C. Chiang, Science **292**, 1131 (2001).
- [3] R. Jaklevic and J. Lambe, Phys. Rev. B **12**, 4146 (1975).
- [4] M. Jalochofski, M. Hoffmann, and E. Bauer, Phys. Rev. Lett. **76**, 4227 (1996).
- [5] C. Wei and M. Chou, Phys. Rev. B **66**, 233408 (2002).
- [6] F. Calleja, M. C. G. Passeggi, Jr., J. J. Hinarejos, A. L. Vazquez de Parga, and R. Miranda, Phys. Rev. Lett. **97**, 186104 (2006).
- [7] R. Otero, A. L. Vazquez de Parga, and R. Miranda, Phys. Rev. B **66**, 115401 (2002).
- [8] F. Calleja, A. L. Vazquez de Parga, R. Miranda, E. Anglada, and F. Yndurain (to be published).
- [9] M. M. Özer, J. R. Thompson, and H. H. Weitering, Nature Phys. **2**, 173 (2006).
- [10] M. M. Özer, J. R. Thompson, and H. H. Weitering, Phys. Rev. B **74**, 235427 (2006).
- [11] D. Eom, S. Qin, M.-Y. Chou, and C. K. Shih, Phys. Rev. Lett. **96**, 027005 (2006).
- [12] Y. Guo, Y.-F. Zhang, X.-Y. Bao, T.-Z. Han, Z. Tang, L.-X. Zhang, W.-G. Zhu, E. G. Wang, Q. Niu, Z. Q. Qiu *et al.*, Science **306**, 1915 (2004).
- [13] A. A. Shanenko, M. D. Croitoru, and F. M. Peeters, Phys. Rev. B **75**, 014519 (2007).
- [14] Y.-F. Zhang, J.-F. Jia, T.-Z. Han, Z. Tang, Q.-T. Shen, Y. Guo, Z. Q. Qiu, and Q.-K. Xue, Phys. Rev. Lett. **95**, 096802 (2005).
- [15] P. Hohenberg and W. Kohn, Phys. Rev. **136**, B864 (1964).
- [16] W. Kohn and L. Sham, Phys. Rev. **140**, A1133 (1965).
- [17] G. Kresse and J. Hafner, Phys. Rev. B **47**, 558 (1993).
- [18] G. Kresse and J. Hafner, Phys. Rev. B **54**, 11 169 (1996).
- [19] J. P. Perdew and Y. Wang, Phys. Rev. B **45**, 13 244 (1992).
- [20] D. Vanderbilt, Phys. Rev. B **41**, 7892 (1990).
- [21] M. Methfessel and A. T. Paxton, Phys. Rev. B **40**, 3616 (1989).
- [22] B. N. Brockhouse, T. Arase, G. Cagliotti, K. Rao, and A. B. Woods, Phys. Rev. **128**, 1099 (1962).
- [23] S. de Gironcoli, Phys. Rev. B **51**, 6773 (1995).
- [24] S. Y. Savrasov and D. Y. Savrasov, Phys. Rev. B **54**, 16 487 (1996).
- [25] Y. Jia, B. Wu, H. H. Weitering, and Z. Zhang, Phys. Rev. B **74**, 035433 (2006).
- [26] A. Ayuela, E. Ogando, and N. Zabala, Phys. Rev. B **75**, 153403 (2007).
- [27] R. Heid, K. P. Bohnen, T. Moritz, K. Kostov, D. Mendel, and W. Widdra, Phys. Rev. B **66**, 161406 (2002).